Clays and Clay Minerals, Vol. 54, No. 2, 165–175, 2006.

HEATING Fe OXIDE-RICH SOILS INCREASES THE DISSOLUTION RATE OF METALS

NICOLAS PERRIER[1,2,3,*], ROBERT J. GILKES[4] AND FABRICE COLIN[1]

[1] IRD UMR 161 and CEREGE UMR 6635, BP A5, 98848 Noumea, New Caledonia
[2] UNC, BP 4477, 98847 Noumea, New Caledonia
[3] Falconbridge, 9 Rue d'Austerlitz, BP MGA 8, 98802 Noumea, New Caledonia
[4] School of Earth and Geographical Sciences, UWA, 35 Stirling Highway, Crawley, WA 6009, Australia

Abstract—Evidence for fire affecting the solubility of metals in Fe oxide-rich Oxisols of the Koniambo Massif of New Caledonia is presented. Acid-dissolution studies showed that Ni, Al and Cr are substituted for Fe in the structure of the Fe oxides. Thermal dehydroxylation of goethite under oxidizing conditions led to the formation of hematite and to the migration of some of these metals towards the surface of hematite crystals as indicated by their enhanced release during the early stage of dissolution. Dehydroxylation of goethite under reducing conditions led to the formation of hematite and maghemite. Nickel and Al were released preferentially during the early stages of dissolution whereas Cr was not released preferentially and may be uniformly incorporated within maghemite and hematite crystals. These results have significance to the mineral-processing industry, to geochemical exploration and to the availability of these metals to plants growing on burnt soils.

Key Words—Goethite, Maghemite, Hematite, Dehydroxylation Acid Dissolution, Lateritic Ore, New Caledonia.

INTRODUCTION

Iron oxides (the generic term used for oxides and oxyhydroxides of Fe) are major constituents of soils of the intertropical belt (Pedro, 1966; Herbillon and Nahon, 1988; Schwertmann and Taylor, 1989). The main Fe oxide minerals are goethite (α-FeOOH) and hematite (α-Fe_2O_3), but minor amounts of pedogenic maghemite (γ-Fe_2O_3) also occur in some tropical and subtropical soils (Taylor and Schwertmann, 1974; Coventry *et al.*, 1983; Schwertmann and Latham, 1986). Various pathways of hematite and maghemite formation have been proposed for both synthetic and natural conditions (Schwertmann and Cornell, 1991; Ruan and Gilkes, 1995). Maghemite may form during pedogenesis by either oxidation of magnetite inherited from parent rock, or conversion of other Fe oxides during soil formation; there is also evidence for a microbial origin of magnetite and possibly maghemite (Rivers *et al.*, 2004). In goethite-dominated soils, maghemite formation may be induced by a combination of heat to dehydroxylate goethite and organic matter to provide reducing conditions that generate Fe^{2+} ions that induce the formation of maghemite rather than hematite (Anand and Gilkes, 1987). Fitzpatrick (1985) and Schwertmann (1985) heated goethite in the presence of organic matter as a reductant to produce maghemite, which is consistent with the natural occurrence of maghemite in soils being the result of bush fires heating topsoil that is rich in organic matter. Recent observations by Anand and Gilkes (1987), Campbell *et al.* (1997) and Grogan *et al.* (2003) of the occurrence of maghemite in soils have come to the same conclusion. Dehydroxylation of goethite in oxidizing conditions leads to the formation of hematite which exhibits structural disorder and retains minor amounts of structural OH in planes perpendicular to the goethite *a* axis (Schulze, 1984; Schulze and Schwertmann, 1984, 1987; Ruan and Gilkes, 1995).

Incorporation of metal ions within the structure of Fe oxides may affect the unit-cell size, particle size and structural order of these minerals, but the fate of these metals during dehydroxylation is not well understood. The literature on Al substitution in natural and synthetic goethite, hematite and maghemite is extensive (Schwertmann *et al.*, 1979; Schwertmann, 1984; Gerth, 1990; Ruan and Gilkes, 1995), but metal substitution is less well documented for other cations such as Cr, V, Ni, Mn, Co that are commonly associated with Fe oxides in soils (Lim-Nunez and Gilkes, 1985; Schwertmann *et al.*, 1989; Schwertmann and Pfab, 1994; Trolard *et al.*, 1995; Manceau *et al.*, 2000; Singh *et al.*, 2002). Due to the occurrence of mixtures of Fe oxides and other minerals in most natural samples, very few studies have investigated the partitioning of metals in Fe oxides in soils and especially the existence of multiple cation substitutions. Similarly, the effects of heating on the location and solubility of metals in soils have received little attention. Soils in arid and seasonal climates frequently experience heating during natural or man-made fires and on ancient landscapes soils may have experienced many episodes of heating (Andersen and Braithwaite, 1992).

* E-mail address of corresponding author:
nicolas.perrier@noumea.ird.nc
DOI: 10.1346/CCMN.2006.0540203

New Caledonia is characterized by the presence of highly weathered Oxisols formed by prolonged weathering of ultrabasic rocks under a seasonal tropical climate (Trescases, 1975), the soils and landscapes are ancient and have experienced frequent exposure to fire (Hope and Pask, 1998). Schwertmann and Latham (1986) showed that maghemite and hematite commonly occur together in New Caledonian soils and also considered that the quite low values of Al substitution in Fe oxides may be due to the low Al content of the parent ultramafic rocks. However, their study did not investigate the incorporation of other metals within the Fe oxides in New Caledonian soils or discuss the impact of heating during bushfires on the mineralogy and chemistry of these soils.

This paper describes the properties of the Fe oxides (goethite, hematite and maghemite) in soils of the Koniambo Massif located in the Northern Province of New Caledonia. Heating experiments with these soils coupled with the results of an acid-dissolution study support the proposal that maghemite and probably some hematite were formed by heating, and also provide an insight into changes in the solubility of isomorphously substituted metals due to heating.

MATERIALS AND METHODS

Samples were obtained from the 0−20 cm horizon of ten soil profiles within the Koniambo Massif and one from the Tiebaghi Massif. Samples A1, A2, A3 and E2 come from ancient soils on the summital surface of the Koniambo Massif (Chevillotte *et al.*, submitted), which is occupied by a dismantled ferricrete. The other soils are distributed along a transect from the summital plateau (900 m above sea level) to a thalweg (700 m). Soil samples B1, B2 and B3 come from a transect on a second surface which consists of a dismantled ferricrete (600 m), extending downslope to 300 m. Soil samples C1, C2 and C3 come from a third surface extending from an altitude of 300 m to the base of the Massif. Soil sample E1 is from the summital surface of the Tiebaghi Massif.

A field survey showed that the coarse fraction is more magnetic than the fine-grained soil; consequently the samples were sieved at 2 mm and the coarse fraction (representing 60% of the total soil, on average) was kept for analysis. A hand magnet was used to separate the magnetic gravel fraction (M) from the non-magnetic gravel fraction (NM) to concentrate the samples with maghemite (Taylor and Schwertmann, 1974). All samples were then ground until all the soil passed through an 80 μm mesh nylon sieve. In order to test the hypothesis of formation of maghemite by heating in bush fires, subsamples of the ground NM fraction were heated in a muffle furnace. Two subsamples were tested, one without any additive (fraction NMB), the other was mixed with 10 wt.% pure cellulose (fraction NMC) representing the organic matter content of the soil. The furnace was heated gradually (30 min) to 600ºC, left at that temperature for 1 h, and the samples were then left to cool gradually in the furnace which returned to room temperature over several hours. This heating regime resembles that occurring naturally in soil adjacent to burning deep litter or fallen wood.

Mineralogical analysis was carried out on all four groups of samples by X-ray diffraction (XRD) using a Philips vertical diffractometer with a diffracted beam monochromator and CuKα radiation. Sodium chloride was used as an internal standard for the measurement of peak position and to indicate instrumental XRD line broadening to enable calculation of crystal size from diffraction line width (Klug and Alexander, 1974). The mean crystallite dimension (MCD) of each Fe oxide was determined from the Scherrer formula (Klug and Alexander, 1974) using the width at half height of XRD lines that were free of interference, and values were calculated using XPAS software (Singh and Gilkes, 1992). For goethites, MCD 110 and MCD 111 were calculated. For hematite, MCD 110 and MCD 104 were measured and MCDc was calculated. For maghemite, MCD 220 was calculated. This choice of reflection is due to many reflections being unavailable due to coincident reflections of the Fe oxides. The hematite/goethite ratio was determined from the XRD peak intensity (peak height × peak width at half height) of the 110 line of hematite (multiplied by 1.43) and the 110 line of goethite. For samples containing hematite, goethite and maghemite, peak overlaps necessitated use of the 012 line of hematite (multiplied by 3.33), the 110 line of goethite and the 220 line of maghemite (multiplied by 3.33). These normalizing factors were determined from XRD data for standard minerals obtained using the same equipment. The Al substitution in goethite was derived from the c dimension of the unit-cell which was calculated using d_{111} and d_{110} values (Schulze, 1984; Novak and Colville, 1989). Aluminum substitution in hematite was derived from the relationship: Al (mole %) = 678 (unit-cell a dimension of nm) (Singh *et al.*, 2000). The Al substitution in maghemite was obtained from the relationship of Schwertmann and Fechter (1984) ($a_0 = 8.343 - 2.22 \times 10^{-3}$ Al (mole %)).

Prior to heating, all samples were analyzed for total chemical composition by X-ray fluorescence spectroscopy after alkaline fusion (in a mix of lithium tetra- and meta-borate as flux) (Norrish and Hutton, 1969). The surface areas of all samples were determined using a Micromeritics Gemini 2375 instrument with N_2 as the adsorbate. For the dissolution kinetics study, 200 mg of each sample (M, NM, NMB and NMC) were shaken at 200 cpm in 200 mL of 1 M HCl in a 500 mL plastic bottle in a controlled environment shaker at 40±1ºC. Successive 10 mL aliquots of the suspension were withdrawn after 1, 2, 5, 20, 45, 80, 165 and 330 h using a plastic syringe, filtered through a 0.22 μm

https://doi.org/10.1346/CCMN.2006.0540203 Published online by Cambridge University Press

Millipore filter (according to the procedure of Singh, 1991) and analyzed for Fe by atomic absorption spectrophotometry (AAS; Perkin-Elmer, Analyst 300) and for other elements using inductively coupled plasma-mass spectrometry (ICP-MS, Perkin-Elmer, PE Elan 600). The total chemical composition of soil samples was determined using an aqua regia dissolution technique followed by analysis by AAS for Fe and by ICP-MS for other elements.

RESULTS AND DISCUSSION

The results and discussion are in three parts, the first part focuses on the mineralogical and geochemical properties of the Fe oxides in the unheated samples, the second part considers the heated samples and the third part examines acid-dissolution congruency and kinetics.

Mineralogical and geochemical properties of Fe oxides

The XRD patterns show that the soil samples are essentially free of silicates, with only traces of lizardite and quartz present in some samples. The samples are predominantly assemblages of three Fe oxides, with much goethite and hematite, together with minor maghemite in most magnetic samples. All non-magnetic (NM) samples contain some goethite and some hematite (with one exception E2NM) while some magnetic (M) samples consist solely of hematite and maghemite (A1M, B2M).

For the M and NM samples, MCD values of goethite crystallites perpendicular to the (110) and (111) planes are ~24.0 nm and 22.0 nm, respectively (Table 1). For hematite in NM samples, 110 and 104 MCD values are ~22.0 nm with only moderate variation (standard deviation of 2.5 nm). The small size of goethite and hematite crystals may be a consequence of substitution of Al for Fe in the hematite structure (Schwertmann *et al.*, 1979). For most M samples, overlapping hematite, goethite and maghemite reflections prevented the measurement of MCD for hematite. The 220 MCD values of maghemite ranged from 25.0 to 56.1 nm with a mean size of 34.6 nm which is much larger than for maghemite in a burnt Queensland soil observed by Grogan *et al.* (2003).

There is no systematic relationship between the values of Al substitution in coexisting goethite and hematite which contrasts with systematic relationships reported by other workers (Schwertmann and Latham, 1986; Singh, 1991; Singh and Gilkes, 1991). This lack of systematic relationship for the present samples could be explained by the presence of other metals (particularly Ni and Cr) as well as Al substitution in the Fe oxides in these soils (Table 2). Multiple substitutions in Fe oxides may result in the incorrect determination of Al substitution from the *d* spacing values which are sensitive to the substitutions of several elements (Gerth, 1990).

Table 1. Mineralogical properties of the Fe oxyhydroxides (a) of the N and M samples, and (b) of the NMB and NMC samples (all values are given as ranges min-max of the series) (N: non-magnetic; M: magnetic; NMB: non-magnetic burned; NMC: non-magnetic burned with cellulose).

a

Samples	magnetic gravel %	Goethite %	Goethite MCD 110 (nm)	Goethite MCD 111 (nm)	Goethite Al (mole %)	Hematite %	Hematite MCD 110 (nm)	Hematite MCD 104 (nm)	Hematite Al (mole %)	Maghemite %	Maghemite MCD 220 (nm)	Maghemite Cell size *a* (nm)	Maghemite Al (mole %)
A1-E2 M	73–20	0–41	16.0–43.3	16.6–30.1	8–14	0–16	18.1–40.5	26.5–27.2	2–8	0–72	25.0–56.1	0.8310–0.8326	8–15
Mean (SD)	38 (16)	26 (22)	25.5 (9.2)	22.5 (4.5)	11 (3)	43 (20)	29.3 (15.8)	26.8 (0.5)	5 (4)	31 (16)	34.6 (11.2)	0.8 (0.0004)	11 (2)
A1–E2 NM		25–100	14.7–36.0	13.9–29.8	9–16	38–75	17.1–25.5	17.1–24.4	4–13				
Mean (SD)		51 (21)	22.3 (6.1)	21.2 (6.0)	12 (2)	49 (21)	22.5 (2.5)	21.6 (2.4)	7 (3)				

b

Samples	% new hematite	% total hematite	Hematite MCD 110 (nm)	MCD 104 (nm)	Al (mole %)	% maghemite	Maghemite MCD 220 (nm)	Al (mole %)
A1-E2 NMBurn	25–100	100	16.7–21.6	10.5–21.8	5–16			
Mean (SD)	51 (21)	100 (0)	18.1 (1.7)	13.5 (3.5)	10 (4)			
A1–E2 NMC	20–67	47–100	13.1–26.1	10.3–21.1	6–14	0–53	20.9–55.2	6–16
Mean (SD)	35 (16)	70 (18)	19.7 (4.4)	14.2 (3.5)	10 (2)	30 (18)	33.1 (10.9)	13 (3)

https://doi.org/10.1346/CCMN.2006.0540203 Published online by Cambridge University Press

The chemical compositions of M and NM samples are listed in Table 2. A statistical analysis enabled identification of affinities between elements and between samples. The principal component analysis (PCA) was performed on the standardized data set for 17 variables (Si, Mg, Ca, Fe, Al, Ti, Mn, Ni, Co, Cr, V, Zn, P, LOI, surface area (SA)) for 22 samples (NM and M fractions). The PCA yields two independent factors explaining 83.4% of the total variance. The first factor, F1, contributing to 62.9% of the total variance is positively associated with Fe, Cr, V and P, and negatively associated with Al, Mn, S.A., Zn, LOI, Co, Ni, Si, Mg and Ca (Figure 1a). Factor F2 contributes 20.5% of the total variance, it is negatively associated with Al, Ti, Mn and P and positively associated with Ca and Mg. Thus

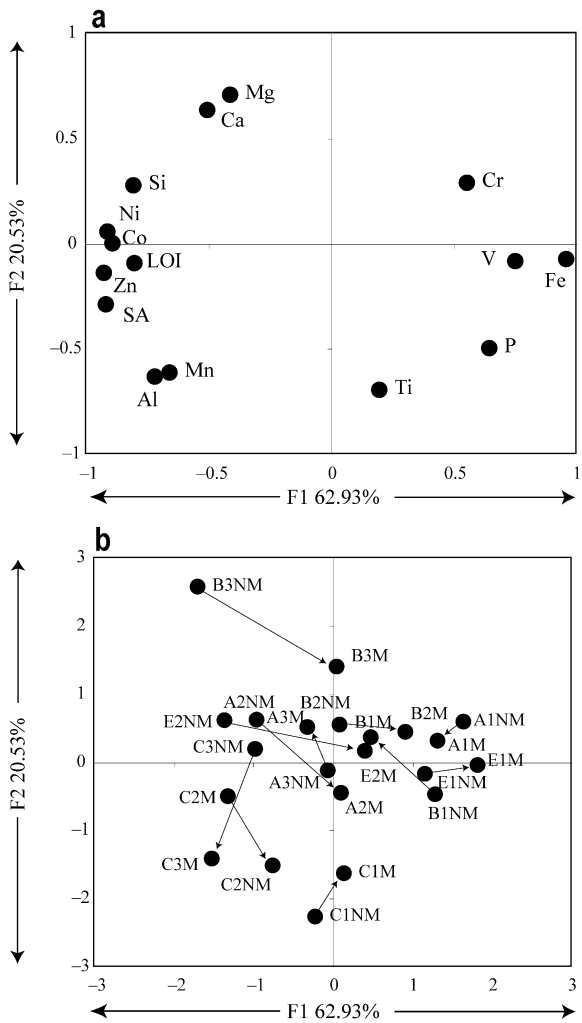

Figure 1. Results of factor analysis carried out on geochemical and mineralogical data for samples of the non-magnetic (NM) and magnetic (M) fractions. (a) Distribution of properties in the F1 *vs*. F2 field. (b) Distribution of samples in the F1 *vs*. F2 field showing linked pairs of N-NM samples. LOI: loss on ignition; SA: surface area.

Table 2. Chemical composition of the samples (all concentrations are given in ranges, min-max of the series).

Samples	Al_2O_3 (%)	SiO_2 (%)	TiO_2 (%)	Fe_2O_3 (%)	MnO (%)	CaO (%)	MgO (%)	P_2O_5 (%)	Cr_2O_3 (%)	NiO (%)	LOI (%)	V (ppm)	Co (ppm)	Zn (ppm)
NM														
A1-E2	3.26–10.24	0.36–18.56	0.08–0.30	86.47–62.18	0.10–1.06	0.01–0.34	0.70–8.66	0.01–0.12	2.13–2.64	0.08–0.75	4.47–14.76	123–430	95–969	80–342
Mean	5.86	5.28	0.16	72.02	0.56	0.06	1.76	0.05	2.38	0.39	11.22	255	564	239
SD	2.00	6.35	0.07	10.54	0.30	0.10	2.33	0.04	0.19	0.23	2.84	89	300	94
M														
A1-E2	2.95–10.26	0.35–9.51	0.07–0.34	64.11–88.93	0.10–1.06	0.02–0.11	0.79–3.35	0.02–0.11	2.09–2.62	0.07–0.60	2.35–11.48	169–462	133–999	56–401
Mean	5.41	3.49	0.17	78.89	0.52	0.04	1.21	0.05	2.37	0.31	6.82	264	531	214
SD	2.73	3.59	0.08	8.82	0.37	0.03	0.74	0.03	0.20	0.21	2.91	91	318	121

https://doi.org/10.1346/CCMN.2006.0540203 Published online by Cambridge University Press

two main metal poles exist, a pole of closely associated Ni, Co and Zn and a more diffuse pole for Fe, Cr and V. Aluminum is not closely associated with either metal pole whereas Si is close to the Ni pole. Figure 1b shows the projection of the samples on the factor score diagram. Except for the quite isolated sample B3NM, the other samples form a continuous population and there is mostly a quite close correspondence between the N and NM pairs of samples indicating that they share a common geochemistry irrespective of their mineralogical differences. This observation supports the proposal that the M samples were formed by heating of NM materials by bush fires.

Heating of samples

In order to reproduce the hypothesized mineralogical and geochemical effects of bush fire on Fe oxides in these soils, the NM samples containing no maghemite and which we assume have not been heated to the same extent as the M samples, were heated with and without organic matter (cellulose). The XRD patterns show distinctly different responses to the two treatments (Figure 2). Without the presence of organic matter all the goethite was transformed into hematite. In the presence of organic matter, the goethite was transformed into both hematite and maghemite as previously reported by Ruan and Gilkes (1995) and Campbell *et al.* (1997) for synthetic Fe oxides and Grogan *et al.* (2003) for naturally occurring Fe oxides. The percentages of new hematite and maghemite formed from the initial goethite were determined by quantitative XRD (Table 1b) and vary greatly between samples.

The 110 MCD value of hematite for heated samples ranges from 13.1 to 26.1 nm (mean 18.7 nm) which is smaller than for the unheated NM (mean 22.3 nm) and M (mean 25.5 nm) samples (Table 1). Similarly the hematite 104 MCD value ranges from 10.1 to 21.8 nm (mean 13.9 nm) for heated samples, smaller than for the unheated samples NM (mean 21.2 nm) and M (22.5 nm). There is a strong linear negative relationship (R^2 = 0.68) between the logarithm of the percentage of new hematite formed and the logarithm of MCD 104 of hematite for the heated samples but no systematic relationship for MCD 110 (R^2 = 0.09) (Figure 3). The relationship for MCD 104 indicates that hematite formed by dehydroxylation of goethite is of smaller size along the *c* axis than was the hematite in the original soils. The MCD for neoformed hematite alone could not be calculated for all samples due to the superposition of diffracted intensities from both neoformed and original hematite but the size of the neoformed hematite is likely to be ~10.0 nm as indicated by the value for E2NMB (10.1 nm) that contains only new hematite. The extrapolated value from the regression line (i.e. to 100% new hematite) is ~9.3 nm which is consistent with this value. During the thermal transformation of goethite to hematite, water molecules are removed in strips running parallel to the *c* axis of goethite and some of the Fe and Al atoms are rearranged in the octahedral interstices (Francombe and Rooksby, 1959). This rearrangement creates voids parallel to the (100) plane of goethite which corresponds to the (001) plane of hematite (Rendon *et al.*, 1983; Watari *et al.*, 1983). The result of this process is the greater sensitivity of the *a* axis of goethite and hence the neoformed *c* axis of hematite, to the presence of excess structural OH (Watari *et al.*, 1983; Schulze, 1984; Schulze and Schwertmann, 1984). Hence MCD 104 values are likely to contract to a greater extent than the MCD 110 values of hematite.

Aluminum substitution for the neoformed hematite ranges from 5 to 16 mole % (mean 10 mole %) and is

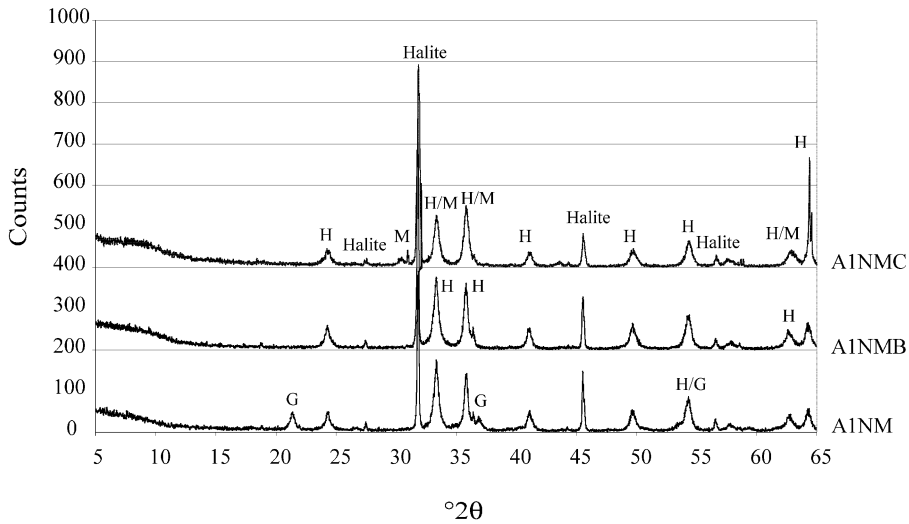

Figure 2. Comparison of XRD patterns of sample A1NM, before and after heating, with and without organic matter. G: goethite; H: hematite; M: maghemite.

https://doi.org/10.1346/CCMN.2006.0540203 Published online by Cambridge University Press

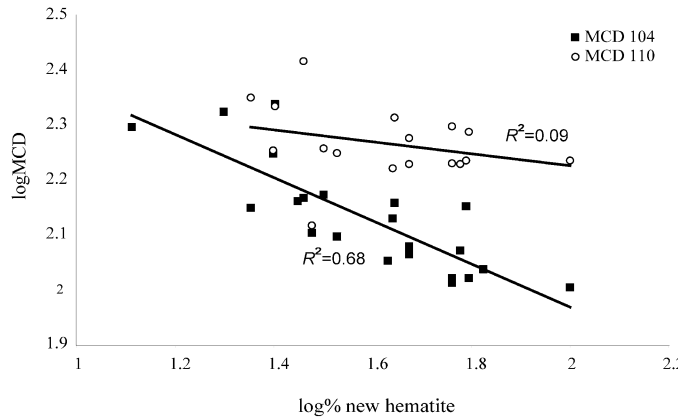

Figure 3. Relationship between the percentage of new hematite in the burnt sample and the mean crystal dimensions perpendicular to the (110) and (104) planes of hematite.

greater than for the unheated NM samples (mean 7 mole %). There is no relationship between Al substitution and MCD (either MCD 110 or MCD 104), which may indicate that the measurement of Al substitution from XRD spacing is not appropriate when hematite contains residual structural OH and various metals (particularly Cr, Ni, Co) as is described below.

For the heated samples, MCD 220 of maghemite ranges from 20.9 to 55.2 nm (mean 33.1 nm), which is similar to the values for the M fraction. However, these values are mostly greater than for the precursor goethites (mean MCD 110 = 22.3 nm), which could indicate that the goethite particles consisted of two or more coherently diffracting zones (Schulze and Schwertmann, 1984), which coalesce during dehydroxylation to form single maghemite crystals (Grogan *et al.*, 2003).

Dissolution studies

Kinetics of Fe dissolution. A dissolution kinetic study of the original and heated samples was undertaken with the dual objectives of determining (1) the congruency of dissolution of metals that may be mostly in the Fe oxide crystals; and (2) how mineralogy and crystal morphology affect dissolution kinetics. Previous studies have shown that metal substitution and crystallinity affect the dissolution kinetics of Fe oxides in strong acids (Schwertmann, 1984; Schwertmann and Latham, 1986; Ruan and Gilkes, 1995).

Dissolution curves commonly follow either the cube root law (Hixon and Crowell, 1931):

$$\sqrt[3]{W} = \sqrt[3]{W_o} - kt \quad (1)$$

where W_o and W are the initial weight and the weight of the sample after time t, respectively, and k is the dissolution rate constant; or the modified Nernst equation (Kabai, 1973; Schwertmann and Latham, 1986):

$$\ln \frac{C_o}{C_o - C} = \alpha \ln k + \alpha \ln t \quad (2)$$

where C_o and C are the initial amount of Fe and the amount of Fe dissolved at time t, respectively, and, α is a constant that is a characteristic of the structure of the solid phase and k is the dissolution rate constant.

Dissolution of Fe from Fe oxides follows more closely the modified Nernst equation (Kabai, 1973) (Figure 4b, Table 3) than the cube root law (Figure 4a). Hence, the cube root law will not be discussed further in this publication.

The dissolution rate constant k for M samples is about twice that for NM samples and the two values are closely positively related (R^2 = 0.62) (Figure 5a). The larger k values (~2.6 fold) for the M samples relative to NM samples maybe due to the presence of maghemite which dissolves more rapidly than goethite and hematite (Xie and Dunlop, 1998). The $k \times 10^3$ values for the NMB and NMC samples are much greater (~7.5 and 10.8-fold, respectively, as indicated in Figure 5b,c) than for the NM fraction but there are no close systematic relationships between k values (R^2 = 0.34 and 0.07). According to Cornell and Giovanoli (1993), hematite dissolves 10 times faster than goethite (which is a major constituent of NM samples and is absent from the heated samples). According to Naono and Fujiwara (1980) and Ruan and Gilkes (1995), hematite formed by dehydroxylation of goethite exhibits high dissolution rates as these crystals contain voids and are structurally disordered. The specific surface area of the heated samples is greater than for the NM samples (mean values for NM – 37, NMB – 70 and NMC – 41 m^2/g). The greater dissolution rates for the NMC relative to NMB samples are thus not a consequence of greater surface area and may result from the presence of maghemite which dissolves more rapidly than hematite as discussed above. Due to the complex assemblages of Fe oxides in the different samples, the combined influence of mineralogy, crystal size, morphology and surface area on dissolution kinetics is complex. Correlation coefficients for the relationships between the logarithm of the rate coefficient of the Nernst equation (Kabai, 1973) and logarithms of several properties of the NMB hematites are given in Table 4. There are strong negative (inverse)

https://doi.org/10.1346/CCMN.2006.0540203 Published online by Cambridge University Press

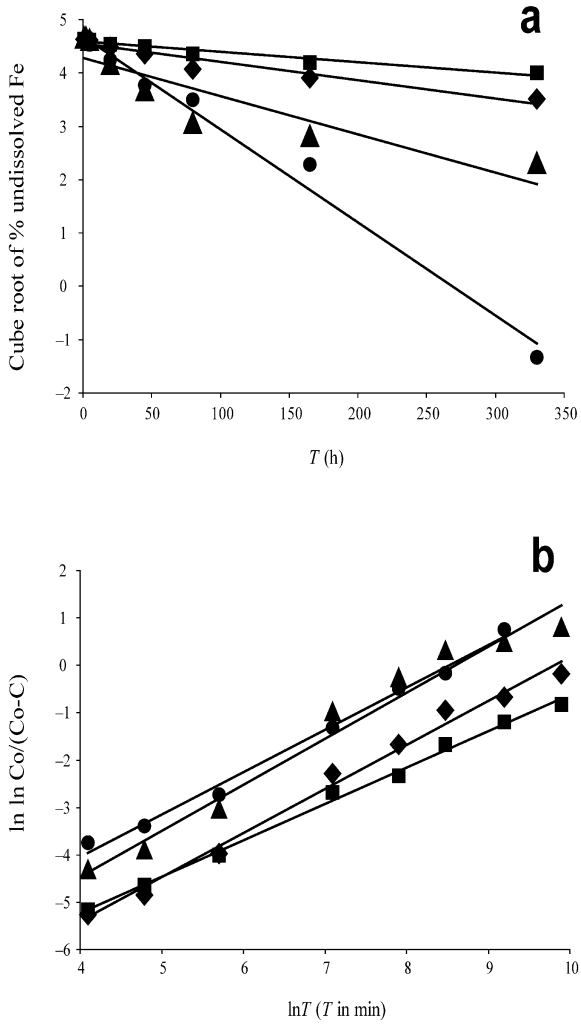

Figure 4. Dissolution curves for samples derived from sample E2 by magnetic separation (M: filled diamond; NM: filled square) and heating in the absence (NMB: filled triangle) and presence (NMC: filled circle) of organic matter. Plots are for the cube root law (a) and the Nernst equation (b).

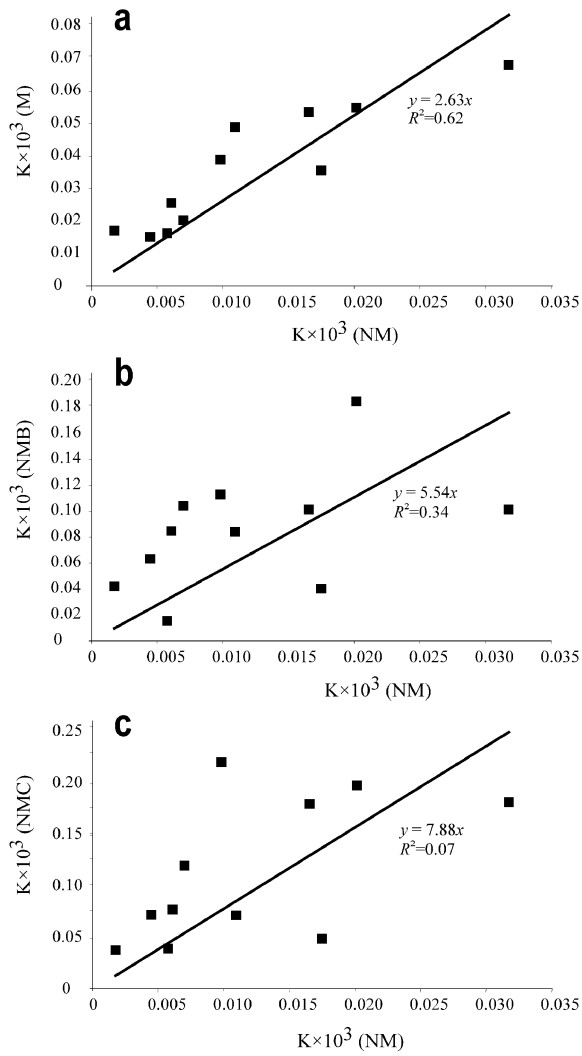

Figure 5. Relationship between values of dissolution rate constant (k) derived from the Nernst equation: (a) for NM and M samples; (b) for NM and NMB samples; and (c) for NM and NMC samples. Fitted lines are constrained to the function $y = m.x$ as intercepts are not significantly different from zero.

relationships between k and both MCD 110 and MCD 104 indicating that small crystals dissolve at a faster rate (Schwertmann, 1984, 1991; Ruan and Gilkes, 1995). However, the four groups of samples do not conform to a common relationship. In particular some NMC samples exhibit much more rapid dissolution (high k) than would be predicted from their surface area but this different behavior is not systematically related to the maghemite/hematite ratio, Al content or crystal size for these samples (Table 1b). There is also a close positive relationship between k and the percentage of neoformed hematite. As discussed above, the neoformed hematite which is a product of dehydroxylation of goethite contains many defects and thus dissolves more rapidly.

Incorporation of metals within the Fe oxides. Goethite and hematite may exhibit isomorphic substitution for Fe by several metals including Al, Cd, Mn, Co, Cr and Ni (Lim-Nunez and Gilkes, 1985; Schwertmann *et al*., 1989; Gerth, 1990). The analysis of the solution for Fe and other metals at intervals during the progressive dissolution of Fe oxides has been used to provide information on the uniformity of incorporation of metals within crystals of magnetite, maghemite, goethite and hematite (Sidhu *et al*., 1981; Lim-Nunez and Gilkes, 1985; Xie and Dunlop, 1998). Plots of the percentage of dissolved metals *vs.* percentage of dissolved Fe are linear, with slope = 1 and with a zero intercept on the ordinate if the metal is uniformly distributed through the Fe oxide crystals (Figure 6 (line i)). If the metal is present both in a discrete and readily soluble form as well as being a constituent of Fe oxide crystals then a significant proportion of the total metal dissolves rapidly

https://doi.org/10.1346/CCMN.2006.0540203 Published online by Cambridge University Press

Table 3. Dissolution rate constant (k) and R^2 for modified Nernst equation plots of dissolution kinetic data for four materials (M, NM, NMB, NMC) (all values are given in ranges, min-max of the series).

Samples	Modified Nernst equation (Kabai, 1973)			Surface area
	α	$k \times 10^3$ (min^{-1})	r^2	(m^2/g)
M				
A1-E2	0.898−1.068	0.0151−0.0681	0.967−0.992	8−57
Mean	0.958	0.036	0.984	30
SD	0.065	0.018	0.008	16
NM				
A1-E2	0.647−0.937	0.0018−0.0318	0.989−1.000	15−48
Mean	0.801	0.012	0.993	37
SD	0.090	0.009	0.004	10
NMB				
A1-E2	0.819−0.980	0.0153−0.1849	0.971−0.993	22−98
Mean	0.913	0.085	0.983	70
SD	0.048	0.046	0.007	22
NMC				
A1-E2	0.742−0.972	0.0402−0.2209	0.980−0.996	14−63
Mean	0.869	0.114	0.989	41
SD	0.070	0.069	0.005	16

before much dissolution of Fe occurs (intercept >0), followed by congruent dissolution (Figure 6 (line ii)). The converse situation where little dissolution of a metal occurs until after a relatively large amount of Fe has dissolved followed by congruent dissolution indicates that a percentage of the metal is in a less soluble form than the Fe oxide (negative intercept) (Figure 6 (line - iii)). Slopes and intercepts of plots of Ni, Al, Cr and Co dissolved *vs*. Fe dissolved for all samples (M, NM, NMB, NMC) are summarized in Table 5. Near congruent dissolution occurred for many samples for Ni, Al and Cr (0.75 < slope < 1.25). For Co, slopes >2 and large intercepts (up to 34.7%) indicate that Co may be at least partly present in a discrete mineral (Figure 6 (line ii)). There is near congruency of dissolution between Mn and Co (*i.e*. slopes of ~1 and intercepts are smaller (~22−25% Co)) indicating the presence of discrete Mn oxides in the samples, which were not detected by XRD. Manganese oxides commonly contain much of the Co present in these soils and their weak crystallinity and low abundance makes them difficult to detect by XRD (Llorca and Monchoux, 1991). For the non-heated samples the intercepts for Ni, Al and Cr are mainly close to 0 indicating an homogeneous distribution of these metals through the Fe oxides (Figure 6 (line i)). Samples B3, C2 and C3, which have intercepts for Ni and Al ranging from 4.37 to 8.77%, contain minor amounts of silicate minerals which may liberate these metals during the early stage of dissolution. For the heated samples the intercepts for Al and Ni increased, indicating that a larger proportion of the metals was at or near the surface of the Fe oxides (Figure 6 (line ii)). The NMC samples, which consist of mixtures of hematite and maghemite, have larger intercepts for Ni and Al than do NMB samples which may indicate a Ni, Al-rich Fe oxide surface or even the presence of a discrete phase (*e.g*. Ni, Al maghemite) that formed during dehydroxylation. For NMC samples, Cr has a negative intercept indicating that it may be concentrated towards the core of maghemite crystals (Figure 6 (line iii)), which may have a greater affinity for Cr than does hematite (Sidhu *et al*., 1980). The relationships between the Ni, Al and Cr intercepts and k for NMB hematites are positive (Table 4), possibly because the hematite structure is disrupted by diffusion of these metals towards the surface of crystals to create a more soluble surface layer. Most of the variation in values of dissolution rate constant k for NMB hematites can be accurately predicted by including all seven measured properties in a multivariate equation:

$$\log k = 2.04 + 0.97X_1 - 2.46X_2 - 0.55X_3 + 0.59X_4 + 0.14X_5 + 0.22X_6 + 0.22X_7 \quad (R^2 = 0.97)$$

where X_1 = log (MCD104), X_2 = log (MCD110), X_3 = log

Table 4. Correlation coefficients (R) for linear relationships between logk (Nernst equation) and log of various properties of NMB samples.

Properties of samples in fraction NMB	log(k)
log(%newHem)	**0.721**
log(S.A.)	**0.882**
log(MCD110)	**−0.648**
log(MCD104)	**−0.932**
log(Ni Intercept)	0.502
log(Al Intercept)	**0.833**
log(Cr Intercept)	0.391

https://doi.org/10.1346/CCMN.2006.0540203 Published online by Cambridge University Press

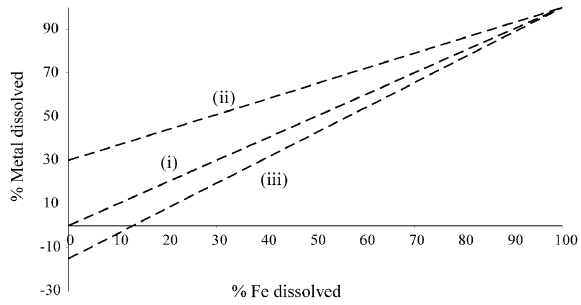

Figure 6. Dissolution of metal elements plotted against Fe for various time intervals: (i) metal is uniformly distributed through the Fe oxide crystals; (ii) metal is present both in a discrete and readily soluble form as well as being a constituent of Fe oxide crystals; and (iii) a percentage of the metal is in a less soluble form than the Fe oxide crystals.

(SA), X_4 = log (% new hematite), X_5 = log (Ni Intercept), X_6 = log (Al Intercept), X_7 = log (Cr Intercept).

A plot of the measured k *vs.* the calculated k showed that there are no systematic deviations from this relationship.

CONCLUSIONS

Gravels in the topsoils of New Caledonian laterite profiles on ultramafic parent rocks are mostly assemblages of three Fe oxides – goethite, hematite and maghemite. The formation of hematite and maghemite in these soils may be due to dehydroxylation of goethite by fire. Hematite may have formed from goethite through heating under oxidizing conditions (without any organic matter) and maghemite by heating under reducing conditions (with organic matter). Acid dissolution results showed that at least three metals (Ni, Al and Cr) were substituted for Fe in the Fe oxides and were distributed quite uniformly throughout the minerals whereas Mn and Co are probably present in a discrete phase. During the thermal conversion from goethite to hematite under oxidizing conditions, some of the Ni, Al and Cr in goethite appears to migrate towards the surface of the neoformed hematite. For samples heated under reducing conditions, Cr does not migrate to the crystal surface and may remain uniformly incorporated in the maghemite Fe oxide structure.

We propose that bush fires may cause some Ni, Al and Cr metals in goethite to migrate to the surface of hematite and maghemite crystals, becoming exposed to soil solution and thus being more available to biota. Frequent repetition of bushfires on ancient land surfaces could therefore substantially alter the availability of these metals to plants.

The result of this research may also be significant to mineral processing, as dehydroxylation of goethitic lateritic Ni may accelerate the dissolution of Ni in hydrometallurgical Ni refineries.

Table 5. Slope (% metal/% Fe) and intercept (% initial content) of dissolution congruency plots for Ni, Al, Cr, Co *vs.* Fe and Co *vs.* Mn for the original and heated samples (all values are given in ranges, min-max of the series).

Samples	Ni *vs.* Fe		Al *vs.* Fe		Cr *vs.* Fe		Co *vs.* Fe		Co *vs.* Mn	
	Slope	Intercept	Slope	Intercept	Slope	Intercept	Slope	Intercept	Slope	Intercept
M										
A1-E2	0.92–1.75	−1.38–8.73	0.77–1.35	−1.07–8.76	1.03–1.17	−2.25 to −0.79	1.02–2.44	−0.62 to −34.76	0.96–1.32	−12.23–1.81
Mean	1.30	0.89	1.07	1.48	1.10	−1.44	1.58	8.31	1.15	−4.46
SD	0.28	3.29	0.18	2.94	0.05	0.55	0.46	10.48	0.14	4.63
NM										
A1-E2	0.74–1.66	−1.72–8.77	0.79–2.22	−0.93–7.13	0.83–1.26	−1.96 to −0.35	0.83–3.52	−1.04–28.71	0.64–1.19	−7.82–1.19
Mean	1.08	0.94	1.36	1.31	1.09	−0.78	1.64	8.37	0.93	−1.90
SD	0.32	3.50	0.42	2.43	0.15	0.51	0.88	9.49	0.19	3.09
NMB										
A1-E2	1.09–1.96	−0.01–15.86	0.76–1.80	−0.05–13.85	0.95–1.30	−1.93–18.46	1.14–2.24	1.28–39.62	0.73–1.58	0.98–25.00
Mean	1.36	6.38	1.28	7.81	1.08	12.93	1.50	15.68	1.05	6.18
SD	0.31	5.73	0.30	4.48	0.13	6.43	0.36	14.38	0.23	7.19
NMC										
A1-E2	0.78–1.24	6.45–33.25	0.79–1.44	2.80–30.30	0.78–1.09	−4.21 to −0.59	0.51–1.70	10.32–83.27	0.87–1.48	−22.47–15.76
Mean	0.97	19.91	1.02	13.15	0.96	−2.38	1.10	35.70	1.12	−5.31
SD	0.17	8.14	0.17	8.51	0.09	0.98	0.36	25.20	0.17	12.29

https://doi.org/10.1346/CCMN.2006.0540203 Published online by Cambridge University Press

ACKNOWLEDGMENTS

The authors thank Falconbridge NC for Nicolas Perrier's PhD grant, the embassy of France in Australia (FEAST program) for travel expenses, Michael Smirk for analytical assistance, Jean-Paul Ambrosi and Anicet Beauvais for corrections, and Professor J. Torrent and an anonymous reviewer for their constructive reviews.

REFERENCES

Anand, R.R. and Gilkes, R.J. (1987) The association of maghemite and corundum in Darling Range laterites, Western Australia. *Australian Journal of Soil Research*, **35**, 303–311.

Andersen, A.N. and Braithwaite, R.W. (1992) Burning for conservation of the Top End's Savannas. Pp. 117–122 in: *Conservation and Development Issues in Northern Australia* (I. Moffatt and A. Webb, editors). North Australian Research Unit, Darwin, Australia.

Campbell, A.S., Schwertmann, U. and Campbell, P.A. (1997) Formation of cubic phases on heating ferrihydrite. *Clay Minerals*, **32**, 615–622.

Chevillotte, V., Chardon, D., Beauvais, A. and Colin, F. Long term geomorphic evolution of New Caledonia Island (Pacific SW). *Terra Nova* (submitted).

Cornell, R.M. and Giovanoli, R. (1993) Acid dissolution of hematites of different morphologies. *Clay Minerals*, **28**, 223–232.

Coventry, R.J., Taylor, R.M. and Fitzpatrick, R.W. (1983) Pedological significance of the gravels in some red and grey earths of central North Queensland. *Australian Journal of Soil Research*, **21**, 219–241.

Fitzpatrick, R.W. (1985) Iron compounds as indicators of pedogenic processes: Examples from the southern hemisphere. Pp. 351–396 in: *Iron in Soils and Clay Minerals* (J.W. Stucki, B.A. Goodman and U. Schwertmann, editors). D. Reidel Publishing Company, Dordrecht, The Netherlands.

Francombe, M.H. and Rooksby, H.P. (1959) Structure transformations effected by the dehydration of diaspore, goethite and delta ferric oxide. *Clay Minerals Bulletin*, **21**, 1–14.

Gerth, J. (1990) Unit-cell dimensions of pure and trace metal-associated goethites. *Geochimica et Cosmochimica Acta*, **54**, 363–371.

Grogan, K.L., Gilkes, R.J. and Lottermoser, B.G. (2003) Maghemite formation in burnt plant litter at East Trinity, North Queensland, Australia. *Clays and Clay Minerals*, **51**, 390–396.

Herbillon, A. and Nahon, D. (1988) Laterites and laterization processes. Pp. 779–797 in: *Iron and Soils and Clay Minerals* (J.W. Stucki, B.A. Goodman and U. Schwertmann, editors). D. Riedel Publishing Company, Dordrecht, The Netherlands.

Hixon, A.W. and Crowell, J.H. (1931) Dependence of reaction velocity upon surface and agitation. *Industrial Engineering Chemistry*, **23**, 923.

Hope, G. and Pask, J. (1998) Tropical vegetation change in the late Pleistocene of New Caledonia. *Palaeogeography, Palaeoclimatology, Palaeoecology*, **142**, 1–21.

Kabai, J. (1973) Determination of specific activation energies of metal oxides and metal oxide hydrates by measurement of the rate of dissolution. *Acta Chimica Hungarica*, **78**, 57–73.

Klug, H.P. and Alexander, L.E. (1974). *X-ray Diffraction Procedures for Polycrystalline and Amorphous Materials*. John Wiley & Sons, New York, 966 pp.

Lim-Nunez, R. and Gilkes, R.J. (1985) Acid dissolution of synthetic metal-containing goethites and hematites. *Proceedings of the International Clay Conference, Denver*, pp. 197–204.

Llorca, S. and Monchoux, P. (1991) Supergene cobalt minerals from New Caledonia. *The Canadian Mineralogist*, **29**, 149–161.

Manceau, A., Schlegel, M.L., Musso, M., Sole, V.A., Gauthier, C., Petit, P.E. and Trolard, F. (2000) Crystal chemistry of trace elements in natural and synthetic goethite. *Geochimica et Cosmochimica Acta*, **64**, 3643–3661.

Naono, H. and Fujiwara, R. (1980) Micropore formation due to decomposition of acicular microcrystals of α-FeOOH. *Journal of Colloid and Interface Science*, **73**, 404–415.

Norrish, K. and Hutton, J.T. (1969) An accurate X-ray spectrographic method for the analysis of a wide range of geological samples. *Geochimica et Cosmochimica Acta*, **33**, 431–453.

Novak, G.A. and Colville, A.A. (1989) A practical interactive least-squares cell-parameter program using an electronic spreadsheet and a personal computer. *American Mineralogist*, **74**, 488–490.

Pedro, G. (1966) Essai sur la caractérisation géochimique des différents processus zonaux résultant de l'altération superficielle. *Comptes Rendus de l'Academie des Sciences, Paris*, **262**, 1828–1831.

Rendon, J.L., Cornejo, J., Dearambarri, P. and Serna, C.J. (1983) Pore structure of thermally treated goethite (α-FeOOH). *Journal of Colloid and Interface Science*, **92**, 508–5116.

Rivers, J.M., Nyquist, J.E., Roh, Y., Terry, D.O. and Doll, W.E. (2004) Investigation into the origin of magnetic soils on the Oak Ridge Reservation, Tennessee. *Soil Science Society of America Journal*, **68**, 1772–1779.

Ruan, H.D. and Gilkes, R.J. (1995) Dehydroxylation of aluminous goethite: unit cell dimensions, crystal size and surface area. *Clays and Clay Minerals*, **43**, 196–211.

Schulze, D.G. (1984) The influence of aluminum on iron oxides VIII. Unit-cell dimensions of Al-substituted goethites and estimation of Al from them. *Clays and Clay Minerals*, **32**, 36–44.

Schulze, D.G. and Schwertmann, U. (1984) The influence of aluminium on iron oxides X. Properties of Al-substituted goethites. *Clay Minerals*, **19**, 521–539.

Schulze, D.G. and Schwertmann, U. (1987) The influence of aluminium on iron oxides XIII. Properties of goethites synthesized in 0.3 M KOH at 25ºC. *Clay Minerals*, **22**, 83–92.

Schwertmann, U. (1984) The influence of aluminium on iron oxides: IX. Dissolution of Al-goethites in 6 M HCl. *Clay Minerals*, **19**, 9–19.

Schwertmann, U. (1985) Occurrence and formation of iron oxides in various pedoenvironments. Pp. 203–308 in: *Iron in Soils and Clay Minerals* (J.W. Stucki, B.A. Goodman and U. Schwertmann, editors). D. Reidel Publishing Company, Dordrecht, The Netherlands.

Schwertmann, U. (1991) Solubility and dissolution of iron oxides. *Plant and Soil*, **130**, 1–25.

Schwertmann, U. and Cornell, R.M. (1991) *Iron Oxides in the Laboratory. Preparation and Characterization*. VCH, Weinheim, Germany, 137 pp.

Schwertmann, U. and Fechter, H. (1984) The influence of aluminum on iron oxides. XI. Aluminum-substituted maghemite in soils and its formation. *Soil Science Society of America Journal,* **48**, 1462–1463.

Schwertmann, U. and Latham, M. (1986) Properties of iron oxides in some New Caledonian Oxisols. *Geoderma*, **39**, 105–123.

Schwertmann, U. and Pfab, G. (1994) Structural vanadium in synthetic goethite. *Geochimica et Cosmochimica Acta*, **58**, 4349–4352.

Schwertmann, U. and Taylor, R.M. (1989) Iron oxides. Pp.

379–438 in: *Minerals in Soil Environments* (J.B. Dixon and S.B. Weed, editors). Soil Science Society of America, Madison, Wisconsin, USA.

Schwertmann, U., Fitzpatrick, R.W., Taylor, R.M. and Lewis, D.G. (1979) The influence of aluminum on iron oxides. Part II. Preparation and properties of Al-substituted hematites. *Clays and Clay Minerals*, **27**, 105–112.

Schwertmann, U., Gasser, U. and Sticher, H. (1989) Chromium-for-iron substitution in synthetic goethites. *Geochimica et Cosmochimica Acta*, **53**, 1293–1297.

Sidhu, P.S., Gilkes, R.J. and Posner, A.M. (1980) The behavior of Co, Ni, Zn, Cu, Mn and Cr in magnetite during alteration to maghemite and hematite. *Soil Science Society of America Journal*, **44**, 135–138.

Sidhu, P.S., Gilkes, R.J., Cornell, R.M., Posner, A.M. and Quirk, J.P. (1981) Dissolution of iron oxides and oxyhydroxides in hydrochloric and perchloric acids. *Clays and Clay Minerals*, **29**, 269–276.

Singh, B. (1991) Mineralogic and chemical characteristics of soils from South-Western Australia. PhD thesis, University of Western Australia, Perth, 200 pp.

Singh, B. and Gilkes, R.J. (1991) Properties and distribution of iron oxides and their association with minor elements in the soils of south-western Australia. *Australian Journal of Soil Science*, **43**, 77–98.

Singh, B. and Gilkes, R.J. (1992) XPAS: an interactive computer program for analysis of powder X-ray diffraction patterns. *Powder Diffraction*, **7**, 6–10.

Singh, B., Sherman, D.M., Gilkes, R.J., Wells, M.A. and Mosselmans, J.F.W. (2000) Structural chemistry of Fe, Mn and Ni in synthetic hematites as determined by extended X-ray absorption fine structure spectroscopy. *Clays and Clay Minerals*, **48**, 521–527.

Singh, B., Sherman, D.M., Gilkes, R.J., Wells, M.A. and Mosselmans, J.F.W. (2002) Incorporation of Cr, Mn and Ni into goethite: mechanism from extended X-ray absorption spectroscopy. *Clay Minerals*, **37**, 639–649.

Taylor, R.M. and Schwertmann, U. (1974) Maghemite in soils and its origin I. Properties and observations on soil maghemites. *Clay Minerals*, **10**, 289–298.

Trescases, J.J. (1975) L'evolution géochimique supergène des roches ultrabasiques en zone tropicale. PhD thesis, Mémoires ORSTOM nº78, Paris, 260 pp.

Trolard, F., Bourrié, G., Jeanroy, E., Herbillon, A.J. and Martin, H. (1995) Trace metals in natural iron oxides from laterites: A study using selective kinetic extraction. *Geochimica et Cosmochimica Acta*, **59**, 1285–1297.

Watari, F., van Landuyt, J., Delavignette, P. and Amelinckx, S. (1983) Electron microscopic study of dehydration transformations III. High resolution observation of the reaction process FeOOH-Fe_2O_3. *Journal of Solid State Chemistry*, **48**, 49–64.

Xie, J. and Dunlop, A.C. (1998) Dissolution rates of metals in Fe oxides: implications for sampling ferruginous materials with significant relict Fe oxides. *Journal of Geochemical Exploration*, **61**, 213–232.

(*Received 26 July 2005; revised 17 October 2005*)